# Accelerated reliability testing of articulated cable bend restrictor for offshore wind applications

Philipp R. Thies*, Lars Johanning, Imran Bashir

*CEMPS - College of Engineering, Mathematics and Physical Science*
*Renewable energy research group, University of Exeter*
*Penryn Campus, Treliever Rd, Penryn, TR10 9FE, UK*

Ton Tuk, Marloes Tuk

*CPNL Engineering GmbH*
*Frohland 4*
*49773 Haren (Ems)*
*Germany*

Marco Marta, Sven Mueller-Schuetze

*Norddeutsche Seekabelwerke (NSW) GmbH*
*Kabelstrasse 9-11*
*26954 Nordenham, P.O.Box 14 64*
*Germany*

**Abstract**

Power cable failures for offshore marine energy applications are a growing concern since experience from offshore wind has shown repeated failures of inter-array and export cables. These failures may be mitigated by dedicated cable protection systems, such as bend restrictors. This paper presents the rationale and the results for accelerated reliability tests of an articulated bend restrictor. The tests are a collaborative effort between the University of Exeter, CPNL Engineering and NSW, supported by the EU MARINET programme.

The tests have been carried out at full-scale and exposed the static submarine power cable - bend restrictor specimen to mechanical load regimes exceeding the allowable design loads in order to provoke accelerated wear and component failures. The tested load cases combined cyclic bending motions with oscillating

*corresponding author, Tel.: +44 (0)1326 255849, Fax: +44 (0)1326 254243
*Email addresses:* P.R.Thies@exeter.ac.uk (Philipp R. Thies*), ton.tuk@cpnl.eu (Ton Tuk), marco.marta@nsw.com (Marco Marta)

tensile forces. A range of acceleration factors have been applied in respect to the 1:50 years load case, subjecting each of the three restrictor samples to 25,000 bending cycles (50,000 tensile cycles). The static power cable was also loaded beyond its intended use, testing the worst case scenario of repeated dynamic loading, purposely inflicting failure modes for investigation. Throughout the test the static submarine power cable sustained over 77,000 bending cycles.

The test demonstrated the integrity of the cable protection system with quantified wear rates obtained through 3D scanning of the individual shells. The static power cable also maintained its integrity throughout the accelerated test regime. None of the failure modes, mainly fatigue cracks and fretting of individual wires, identified by cable dissection would have caused a direct loss of service. The observed failure modes could also be predicted through numerical load analysis, giving confidence in the utilised mechanical modelling and cross-sectional analysis for dynamic applications.

*Keywords:* accelerated testing, cable protection, offshore renewable energy, submarine power cable, reliability

---

## Contents

## 1. Introduction

Offshore wind energy has reached a stage where it is a substantial part of the installed generation capacity, with ambitious plans to further increase its share. The UK is currently the world leader with 3.7GW of installed and grid connected offshore turbines (as of end 2013) being part of a total of 48GW offshore wind projects in operation and under development [1]. As of July 2014, the combined capacity of grid-connected offshore wind projects in European waters amounts to 7.3GW [2].

The industry is under increased scrutiny to achieve competitive levelised cost of electricity favourably below the symbolic £100/MWh mark in the mid (2020) to long-term (2050) [3]. One of the crucial factors to achieve this is high system reliability to ensure high operational availabilities with target levels above 97%. The system reliability level of onshore wind turbines which is in the order of 2.4 failures per turbine per year [4] has to be matched or improved in order to achieve economically viable availability levels [5]. A recent study [6] for offshore wind turbine reliability data calculates 8.3 failures per turbine per year.

One of the emerging challenges to achieve these high availability levels is the reliability of inter-array and export cables. A recent industry estimate [7] is that whilst only about 10% of the capital expenditure for offshore wind installations is associated with the cable cost, 90% of reported insurance claims are attributed to cable failures. Failure consequences incur both plant downtime as well as considerable replacement and repair cost. Failure rate levels for onshore medium voltage cables range typically between 2-3 failures per 100km per year, whilst some UK offshore wind installations report failure rates between 5-8 faults per 100km per year [8]. The problem is exacerbated by the fact that offshore locations increase unplanned maintenance cost for cable faults by a factor of 10 to 100, compared to onshore incidents.

The root causes of cable failures are reported [8, 9] to be a combination of poor installation practice, inadequate design of the cable itself and related accessories as well as inadequate mechanical protection for the given environmental

load conditions. Apart from the first cause, the failure mechanism is driven by the wave and tidal/current interactions with exposed cable sections, causing external abrasion and mechanical wear as well as cyclic bending, resulting in premature cable failures.

Accelerated testing seeks to increase component stress levels with the assumption that the damage accumulates over the lifetime of the component. The objective is to accelerate the time needed to observe failure modes by using test regimes which are representative of the conditions expected in the field [10]. These types of tests allow to test the long-term behaviour of components within feasible cost and time budgets. The benefits of accelerated testing to obtain more accurate reliability predictions despite limited operating experience are described in [11]. More specifically [12] have carried out performance comparison tests for mooring lines under accelerated loading conditions. A number of studies also report the dedicated testing of submarine power cables. A review of typical mechanical tests for submarine dynamic power cables is presented in [13]. Further detailed studies focussing on the fatigue failure of the copper conductors of marine power cables have been carried out by both numerically [14] and experimentally [15, 16]. The authors are not aware of any study that reports the behaviour of a dynamic power cable armoured with a cable protection system.

A number of companies have developed cable protection systems that aim to prevent cable failures. An extensive review of cable protection measures is given in [17, 18] describing the range of installation techniques and available cable protection systems. The main length of the subsea cable is buried where possible. The burial depth is depending on the seabed conditions, installation method and on the exposure risk of the cable, incl. fishing, vessel activity, waves and tides and is typically quantified by the Burial protection index (BPI) [19]. Where the cable cannot be buried alternative protection measures have to be taken, such as concrete mattresses, rock dumping or cable protection systems. Bend restrictors are one example of cable protection systems and will be the focus of this paper.

Cable protection systems (CPS) are commonly used in the oil and gas and offshore wind industry to prevent damage to an umbilical cable (or riser) from overbending. There are two types of CPS, *bend restrictors* and *bend stiffeners*. Indicative drawings are shown in fig. 1.

*Bend restrictors* (fig. 1(a)) usually comprise a number of interlocking elements which are compliant until a specified bend angle/bending radius, greater than the MBR of the cable, is reached. The elements thus protect the cable from overbending. The bend limiter accepts the bending moments, once the design angle / bend radius is reached. They are best suited to protect the cable during installation and operation in static or quasi-static conditions.

*Bend stiffeners* (fig. 1(b)) are tapered mouldings that add local stiffness to cable or umbilical to limit the bending stresses and curvature to acceptable levels, avoiding failures due to fatigue and overbending. They are best suited for dynamic applications to control/reduce the in-service bend radius to achieve a specified service life. This design provides local stiffness to the cable, thus limiting bend stresses, fatigue and curvature. The bending stiffener body is commonly made from polyurethane elastomers.

The focus of this paper is on a particular type of bend restrictors, the so called articulated pipe or "split pipe" design. In addition to cable protection from overbending, the articulated pipe design also provides both additional dynamic stability due to the significant mass of each component and a robust protection against impact failures that may be caused, for example during rock dumping. Articulated pipes also offer cable protection in situations where the cable cannot be buried, as well as during installation procedures, such as off-loading or cable pull-in. The split pipe design refers to the two half-shells that form a member of the articulated pipe. They can be directly assembled to the cable before installation or can be mounted by divers once the cable has been laid, i.e. retrofitted to existing installations.

This paper presents the rationale and the results for accelerated reliability

tests of a full-scale cable & bend restrictor section. The tests were funded under the EU MARINET programme and are a collaborative effort between i) the University of Exeter (UK), ii) CPNL Engineering (Germany) and iii) NSW (Germany); providing i) the Dynamic Marine component test rig as test facility, ii) the bend restrictors and iii) the static power cable.

The paper falls into five sections. Following the introduction (sec. 1) the experimental setup and the test specimens are described in detail in sec. 2. This includes a description of the test rig itself as well as the CPNL cable protection system and the static submarine power cable, supplied by NSW. Typical operational load cases have also been modelled. Section 3 gives a summary of the main test results, comprising test observations as well as post-test quantification of wear rates and failure mode assessment. The results are discussed in sec. 4. Conclusions and further work are given in sec. 5.

## 2. Experimental test setup & Load regimes

This section sets out the experimental setup including the test rig where the work has been carried out and the test specimen in form of the cable protection system and the power cable. A view to what load conditions are expected for offshore wind applications is also presented. This will allow to set the accelerated tests into the operational context. It should be noted that all of the applied test loads were well above the allowable design loads for both the cable protection system and the submarine power cable. As will be shown, the test regimes range between 0.22 to 6.67 times the 1:50 years extreme load event for given offshore wind installations. This 1:50 load event was then repeated with 25,000 bending cycles (50,000 tensile cycles) for each of the three tested cable protection samples, whilst the static power cable was dynamically loaded with over 77,000 bending cycles. As such, failure modes were deliberately provoked in order to explore the component integrity limits. The post-test analysis of components was based on visual inspection and 3D scan results. Some degradation of the components mechanical properties due to both wear and cracks on metallic

surfaces caused by fatigue was expected. The test objective was to ensure the integrity of the CPS would is not compromised under the applied loads, whilst fulfilling its function to protect the cable from mechanical failures.

### *2.1. Dynamic Marine component test rig (DMaC)*

The tests have been carried out on the Dynamic Marine Component test rig (DMaC) at the University of Exeter. The main objective of the test facility is to replicate the marine environmental load conditions as closely as possible. The rig facilitates the dynamic testing of large-scale components in a controlled environment applying realistic motion and/or load characteristics. The main feature that is benefitting the tests presented in the following is the capability to simultaneously apply bending moments and axial forces. The bending moment is applied by the moving headstock which allows a bending angle of $\pm 30°$ in two planes, whilst the tailstock can apply a given axial dynamic load signal up to 23tonnes. The rationale of the service simulation testing approach and the implementation of the rig is described in more detail in [20–23]. An overview of the experimental setup, showing both the axial tailstock and the headstock is shown in fig. 2.

### *2.2. Cable protection system*

The CPNL cable protection system is used to protect submarine power cables against overbending and excessive forces during the installation phase and throughout the operational life-time. This articulated pipe bend restrictor solution comprises of individual elements that interlock into a shell of 2 elements, which in turn can be assembled in a string of elements to surround and protect a power cable. The dimensions of the individual and assembled elements are shown in fig. 3. The material of the segments is cast iron EN-GJS 400/15 with a UTS of a segment at 18% that of the material property. The specimen used in the tests comprised of 30 individual elements (15 assembled shells) with a total length of $L = 5.4m$. Figure 3 shows the dimension and assembly of the articulated pipe cable protection system.

*Modelled load cases for cable protection system.* In order to relate the environmental load conditions to the test regime the anticipated load cases have been modelled numerically using the proprietary software OrcaFlex [24]. The main modelling parameters for the submarine power cable and the CPS are shown in tab. 1. The focus of this initial analysis lies on the maximum load conditions likely to be encountered for offshore wind farm installations, where cable and CPS system are fed through a J-tube into the tower. The force experienced by the CPS system is a function of its free-span length which in turn is a function of the scour depth. The worst case scenario considering scouring was modelled under the following assumptions, see also fig. 4:

- The burial depth of the cable and the CPS is $d_{burial} = 2m$.
- The global scour is set to $S_{global} = 1m$ and
- The diameter of the monopile is $D = 5m$
- The expected scour depth, $S_{depth}$ is calculated as:
  $S_{depth} = 1.3 \cdot D = 1.3 \cdot 5m = 6.5m$
- The influence of the monopile & J-tube on the flow regime is not considered.
- The current and wave direction are collinear.

A total of six different wind farm locations have been considered with a range of water depths, 1:50 year wave conditions, and surface current velocities as given in tab. 2. Additionally, the wave/current directions (45-135°), the seabed friction coefficient (0.1 - 0.5), the boundary stiffness with the soil (zero/infinite) and the residual tension after cable-lay (1-15kN) have been varied for all cases.

The maximum force on the CPS has been observed at the location of the cable clamp centralizer, which is situated in the monopile/J-tube bell mouth. The maximum load conditions across the range of sites and cases are presented in table 3. The highest shear forces and local bending moment occurred for location 3 whilst the highest axial force is noted in locations 2/3. The influence of the

Table 1: Properties of submarine power cable and cable protection system for modelled load cases. Please note: Cable properties for modelled case differ from tested cable (see also table 5)

**Submarine power cable**

| Cross-section | Immersed weight | Diameter | MBR | Max tension | Axial stiffness | Bend stiffness |
|---|---|---|---|---|---|---|
| [$mm^2$] | [kg/m] | [mm] | [m] | [kN] | [MN] | [kN.m$^2$] |
| 150 | 15.90 | 110 | 1.65 | 80 | 192 | 2.8 |

**Cable protection system**

| Type | Immersed weight | Inner diameter | Outer diameter | MBR | Bending angle | Max tensile strength |
|---|---|---|---|---|---|---|
| | [kg/m] | [mm] | [mm] | [m] | [°] | [N/mm$^2$] |
| CP137-333 | 39.84 | 137 | 213 | 2.54 | 4.75 | 400 |

Table 2: Modelled load cases covering different wind farm locations

| Location | Water depth | Wave height | Wave period | Current velocity |
|---|---|---|---|---|
| | [m] | ($H_s/H_{max}$) [m] | [s] | [m/s] |
| 1 | 27.8 | 8.1/15.1 | 9.1 - 13.3 | 1.26 |
| 2 | 22.7 | 8.1/15.1 | 9.1 - 13.3 | 1.26 |
| 3 | 19.4 | 8.1/15.1 | 9.1 - 13.3 | 1.26 |
| 4 | 9.8 | 4.1/7.6 | 7.0 - 9.7 | 1.14 |
| 5 | 11.9 | 5.0/9.3 | 7.8 -10.1 | 1.60 |
| 6 | 19.2 | 7.4/13.8 | 9.5 - 14.2 | 1.50 |

Table 3: Maximum load results between monopile/J-tube and CPS

| CPS | Shear $F_{max}$ [kN] | Axial $F_{max}$ [kN] | Bending $M_{max}$ [kN.m] |
|---|---|---|---|
| CP137-333 | 15.61 | 11.58 | 12.35 |

modelled soil friction coefficients is minimal. However the results are influenced by the boundary stiffness between the CPS and the soil. The presented results assume the worst case with a pinned connection (zero stiffness), as opposed to an encased infinite stiffness. Similarly, the largest loads occur in situations with the highest residual tension of 15kN and in conditions where the waves and currents act perpendicular on the CPS (90° case).

### *2.3. Static submarine power cable*

A three phases AC 18/30 kV sample static power cable section was supplied for the test. It includes 3x240mm$^2$ round copper conductors and a 48 single mode fibre optics element. It is representative of a wind farm inter-array subsea power cable design. The cable is designed to withstand - within the stated limits - the variable tensile loads and bending that occur during handling, laying and possibly retrieval. Mechanical loading limitations are stated and tested according to Cigre/Electra 171 recommendations [25]. The cable would normally be laid in trenches or suitably protected from overbending, crushing or excessive tensile load. It is not designed to withstand significant variable loading during operations. For these applications, an appropriately designed dynamic power cable should instead be selected. A summary of the most relevant mechanical characteristics is given in tab. 5 and a detailed compound drawing is shown in tab. 4. A short description is also provided in the next sections.

*Power core design, components and assembly.* The cable includes three power cores following the CENELEC HD 620 standard [27] with 240 mm$^2$ IEC Class 2 [28] stranded and compacted copper conductor. Longitudinal water tightness through the conductor is achieved through longitudinal semi-conducting

Table 4: AC 18/30 kV; 3×240mm$^2$ round copper conductor power cable: Cable components, after [26]

| **Medium Voltage AC Submarine Power Cable** | |
|---|---|
| 3 × 240 mm$^2$ Cu 18 / 30 kV - 48 SM FO element | |
| 1 | Fibre-optic element |
| 2 | 240 mm$^2$ round conductor, water blocked |
| 3 | Inner semi-conductive layer |
| 4 | XLPE insulation |
| 5 | Outer semi-conductive layer |
| 6 | Swelling tape |
| 7 | Copper wires screen |
| 8 | Copper tape counter helix |
| 9 | Swelling tape |
| 10 | Metallic sheath |
| 11 | Outer sheath |
| 12 | Round fillers |
| 13 | Bedding layer |
| 14 | Galvanized steel wires filled with bitumen compound |
| 15 | PP yarn cladding |

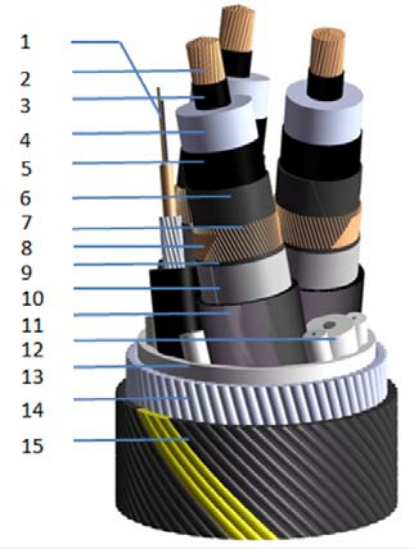

hygroscopic tapes (swelling tapes) and threads. The triple extruded polymer insulation system is rated for the voltage 18/30 (36) kV at 50/60 Hz. It consists of a semi-conducting conductor screen, a cross-linked polyethylene (XLPE) insulation and a semiconducting insulation screen [29]. Semi-conducting hygroscopic tapes (swelling tapes) are wrapped around the semi-conducting insulation screen. It provides the bedding for a copper wire earth screen topped by a counter helix copper tape and a further layer of semi-conducting hygroscopic tape. The power core sheathing system is composed by an aluminium layer fully bonded to a high density polyethylene (HDPE) layer to provide full permeability to radial water penetration as well as suitable mechanical protection. The cable also includes 48 single mode fibres (SMF) in a copper buffer tube. Steel wires armouring and HDPE sheath are applied for mechanical protection.

The cable cores are laid up according to a semi-wet design in which the sea water can penetrate up to the HDPE sheath of the individual cores. Gaps within the cable twisted cores bundle are filled with round PE filler elements. One of the interstitial fillers is replaced by the fibre optics element. Cores and interstitial fillers are tied together using a bunch of aramid strings and topped by a non-conductive bedding layer that has the double function of presenting a regular round surface for armouring wires stranding as well as protecting the core bundles.

A single layer of galvanized steel provides both mechanical protection and tensile strength. The layer is flushed with bitumen. Finally, a layer of polypropylene yarn is applied over the armouring layer for wear protection as well as ensuring that anti-corrosion protection is not compromised during either handling or laying.

Table 5: AC 18/30 kV; 3x240mm$^2$ round copper conductor power cable - key parameters

| Parameter | Value |
|---|---|
| Nominal overall cable diameter | 123 mm |
| Max. recommended pulling force | 60 kN |
| Recommended minimum bending radius | 2.5 m |

### *2.4. Fixtures & sample installation*

The test sample was fitted into the DMaC using attachments pieces to connect the articulated pipe with the backing plate of the headstock as well as to the tailstock, see fig. 2. At the headstock end, the cable was fed through the connection and the armouring was clamped against the backing plate using M24 bolts as shown in fig. 2(c). Once the cable was connected, the CPS shells were fitted around the cable and terminated at the tailstock end using semi-circular clamping plates (fig. 2(b)). As such, the power cable was fixed only at the headstock whilst it was free to slide in and out at the tailstock connection, allowed to move independently to the bend restrictor string. The individual power cores were fed down around the crossed shaft of the Zram attachment plate. The bend restrictor shells were numbered from 1-30, starting from the tailstock. A total of three bend restrictor samples were tested: sample A (labelled from 1-30); sample B (labelled B1-B30) and sample C (labelled C1-C30). The cable remained into place when changing the CPS shells.

### *2.5. Test specifications & load regimes*

Over the duration of the test three samples (A, B, C) have been exposed to four different load cases, varying both the tensile force and the bending angle.

The investigated cases aimed to replicate the conditions the power cable / bend restrictor is likely to experience, once significant scour around the pile has taken place. The increased free span will cause an increased tension at the J-tube exit, which is the reason for the tensile force at 0° bending angle. Once the CPS has an increased free span, it is also susceptible to transverse bending,

induced by the tidal flow. The phase relationship was chosen to replicate the oscillation between maximal axial load, due to the free span at 0° bending and maximum 28° bending angles at reduced axial tension. Failure modes of concern were in particular the wear and fatigue cracking of the bend restrictors and any mechanical failure of the power cable components due to either extreme or fatigue loading.

Table 6 gives a summary of the tested samples, specifying the load envelopes and accumulated number of cycles. Figure 5 shows a time series of the measured bending angles and tensile force for load case 1.1, simultaneously applying both in an alternating manner. The tensile load varied between 80kN and 20kN, with bending angles (y-axis) of ±28°. The phase relationship between the tensile force (Z-ram) and the headstock is such that the maximum axial tension occurs at zero bending of the headstock and the minimum axial load occurs at maximum and minimum bending angle of the headstock. Each cycle has a time period of 4.32s and 8.64s at the Zram and headstock respectively. Each test consists of 833 cycles at the headstock and the duration for each test was two hours. The test was carried out with bend restrictor sample 'A' and the total number of cycles achieved with load case 1.1 was 1,167.

Similarly, load case 1.2 was used to test bend restrictor sample 'A+'. In comparison to load case 1-1, it had a reduced tensile load varied between 15 kN and 10 kN, with reduced bending angles (y-axis) of ±14°. A total of 25,014 cycles at the headstock were achieved using load case 1-2. Load case 2 was used for sample 'B', with an increased tensile load varied between 20kN and 15kN and identical angles as compared to load case 1.2. Due to the smaller bending angles, the period was reduced by 1/3rd in order to speed up testing. The load replication was not influenced by this change. Load case 3 was used to test sample 'C', at same tensile force, but lower bending angles as compared to load case 2. A total of 24,990 bending cycles was achieved for load case 2 and 3.

Table 7 relates the applied loads to the estimated extreme loads (1:50 yr event) during operation. It should be noted that the stated acceleration factors only relate to the extreme event. The tensile load acceleration factor (AF) was

Table 6: Summary of test specifications, stating samples, load case and number of accumulated cycles

| Name | Axis | Maximum | Min | Total cycles | Cycle period |
|---|---|---|---|---|---|
| **SAMPLE A (Shells 1-30)** | | | | | |
| Load case 1.1 | Zram | 80kN | 20kN | 2334 | 4.32s |
| | Head stock y | 28° | -28° | 1167 | 8.64s |
| *Shell 29 & 30 failed and were replaced with 31 & 32* | | | | | |
| **SAMPLE A+ (Shells 1-28, 31, 32)** | | | | | |
| Load case 1.2 | Zram | 15kN | 10kN | 45028 | 4.32s |
| | Head stock y | 14° | -14° | 25014 | 8.64s |
| **SAMPLE B (Shells B1-B30)** | | | | | |
| Load case 2 | Zram | 20kN | 15kN | 49980 | 2.88s |
| | Head stock y | 14° | -14° | 24990 | 5.76 s |
| **SAMPLE C (Shells C1-C30)** | | | | | |
| Load case 3 | Zram | 20kN | 15kN | 49980 | 2.88s |
| | Head stock y | 7° | -7° | 24990 | 5.76 s |

varied from 6.67 to 1.25 to 1.67 for the three load cases, whilst the bending moment reached AFs of 0.54, 0.28, 0.22 and 0.22 for the four load cases. The acceleration of bending moments was constrained by the max bending moment that could be applied by the test rig.

## 3. Test results

### *3.1. Test observations*

*Load case 1.1.* Bend restrictor sample A was tested under the conditions outlined in load case 1.1. The first test was completed in two hours during which the sample was exposed to 833 cycles in bending and 1,666 cycles of axial loading. During the second test the failure event occurred at 330 bending cycles. The connecting bend restrictor thus failed after a total number of 1,163 bending cycles and 2,326 axial cycles under accelerated load case 1.1. The failure occurred close to the headstock where the restrictors were exposed to maximum bending angle. The shells that broke were located at the end sections connect-

Table 7: Relating numerical load calculations to DMaC experimental load regimes - Acceleration factors

| Max moment/force | | Load case | Acceleration Factor (AF) |
|---|---|---|---|
| **Tensile axial force** | | | |
| $F_{max}$ [kN] | | | $F_{DMaC}/F_{Max,model}$ |
| Numerical | DMaC | | |
| | 80 | 1.1 | $AF_{T1.1} = 6.67$ |
| ≈12 | 15 | 1.2 | $AF_{T1.2} = 1.25$ |
| | 20 | 2 & 3 | $AF_{T1.2} = 1.67$ |
| **Bending moment** | | | |
| $M_{max}$ [kNm] | | | $M_{DMaC}/M_{Max,model}$ |
| Numerical | DMaC | | |
| ≈13 | $7.0^{(*)}$ | 1.1 | $AF_{B1.1} = 0.54$ |
| | 3.6 | 1.2 | $AF_{B1.2} = 0.28$ |
| | 3.3 | 2 | $AF_{B1.2} = 0.25$ |
| | 2.9 | 3 | $AF_{B1.2} = 0.22$ |

$^{(*)}$ Estimated value, due to logging error. Test rig operated at maximum capacity, which is known.

ing the sample string to the headstock. The failure was on the lip of the shells that locks over the lip on the stainless steel attachment piece.

After this failure the pieces were removed from the test rig and analysed closely. The cause of this failure was attributed to the stainless steel-cast iron contact of the shell-headstock interface connection. The two shells (A29 and A30) were exposed to considerable wear and abrasion with visible abrasion residue. This failure was ascribed to the point loading applied by the test rig. It was deemed an unrepresentative failure mode for the CPS exiting the J-tube from a monopile. The bending loads induced by tides and/or waves would be distributed along the length of CPS.

*Load case 1.2.* Following this failure event, the load case specifications were reviewed and adjusted to make a more representative test case. The broken shell specimens were replaced, and the refitted sample A was subsequently exposed to load case 1.2, which was completed without any failure. However, the bend

restrictors showed some wear and tear. Again, like load case 1.1, the maximum abrasion was observed near the head stock at maximum bending angle.

*Load case 2 and 3.* Load cases 2 and 3 were completed without any failure. Some limited wear and abrasion were observed near the headstock.

### *3.2. CPS Scanning*

Following the test completion the articulated pipes were carefully disassembled and transported to undergo a 3D scan using the triple scan technology [30] to compare the CAD image with the tested specimens. This allows a visual and quantified assessment of the amount and locations of wear for the different test regimes. The CAD image and the scanned image have been aligned along its three principal axes. This then allowed quantifying the deviation, i.e. the incurred wear for each individual shell. An example of a scanned shell is depicted in fig. 6. These scans were taken as the basis to infer the maximum wear for each cell. A summary of estimated wear is plotted in fig. 7. Only the shells close to the headstock / tailstock were scanned for each sample. It can be seen that sample A has the largest wear with 0.6mm across all shells, followed by sample B with 0.2mm wear near the tailstock and 0.4mm wear near the headstock. Sample C has the lowest wear with 0.1 mm and 0.4 mm respectively. Given the number and severity of load cycles the wear is very modest and demonstrates the integrity of the CPS design under the given loads. The original wall thickness of the shells is 8mm, with a critical wall thickness of 5mm.

### *3.3. Cable analysis*

#### *3.3.1. Numerical analysis*

A numerical cross section analysis has been carried out with the use of the finite element analysis (FEA) application CableCAD [31], which is a design and modelling software aimed at the analysis of cables [32]. It includes a graphical user interface that makes both the drawing of complex cable configurations and the definition of the loads parameters a relatively simple process. The program produces a meshed finite element model where individual components

like wires, strands, jackets or sheaths are represented as macro-element. An element stiffness matrix is generated for the each contact points between adjacent components, defined as macro-nodes. The prediction of slip for locked and meshed helical components is based on contact forces at the layer inner and outer diameters. Both static and kinetic friction coefficients are defined as material properties. When macro-nodes stiffness matrices are generated, then system loads are applied to yield displacements, deformation and stresses for the cable components.

The mechanical analysis was based on actual measured values recorded during cable inspection rather than specification/production plans. Following the test conditions, it was assumed that the applied bending is almost completely transferred to the power cable, while axial load acting on the cable is considered as minimal, i.e. limited to the friction force as the cable was allowed to slip inside the bend restrictor. In order to carry out the mechanical analysis, the DMaC headstock y angles had to be converted to cable global curvature. The estimate was based on images and videos, as well as measurements of the components' geometry. Bending radii were estimated at approximately 2.0m, 3.5m and 7.0m for, respectively 28°, 14° and 7° headstock y angles.

*Maximum effective stress.* This is calculated through CableCAD analysis. It is the maximum von Mises stress occurring within a cable layer. Von Mises effective stress is a single uniaxial stress equivalent to the stress state produced by complex loading conditions. This method evaluates the failure occurrence under complex conditions of stress based on the results of simple uniaxial tensile test. It is commonly applied to the failure mechanism analysis of metals [33]. Here it is applied to assess the effects of both extreme and fatigue loading. For the given load cases, the maximum effective stress for all cable components was calculated. This is given by the summation, following the von Mises criterion, of the stress effects of all loads acting on an element.

*Extreme loading.* For the extreme load cases applied, no significant impact was expected in any of the polymeric elements, while the result for all metallic

components is shown as a percentage of the material yield strength in tab. 8.

With the given cable loading assumptions the following can be concluded: The stress acting on the aluminium sheath is estimated as 65% of yield strength limit at 28° bending. Accounting for possible high stress spots due to uneven load distribution, the probability of extreme load failure is estimated as medium. The stress acting on the copper tape is approximately 35% of the yield strength limit at 28° bending. The probability of extreme load failure is deemed to be low.

At 28° bending, the stress acting on the armouring wires was estimated as 25% of the yield strength limit, while for the inner cable metallic components the calculated stress was only a small fraction of the material yield strength. The likelihood that these components will fail due to extreme loading is small.

*Fatigue loading.* The second load condition of concern, in particular in the marine environment, is fatigue [34, 35]. The tests applied regular cyclic load regimes which allow to assess the fatigue performance of the cable. The fatigue life of each cable component is estimated by referring both the Maximum Effective Stress as computed by the CableCAD software and the number of cycles applied in each load case to the materials S-N curves and following Miners linear damage accumulation principle [36]. The estimated accumulated fatigue damage for the total cycles applied in the test load cases indicates that fatigue failure of both metallic screen copper tape and aluminium sheath is highly likely. Figure 8 plots the number of stress cycles against the stress amplitude for the 28° bending angle, together with the relevant design S-N curve [37, 38]. It shows that considerable damage, beyond the endurance limit of the S-N curve was accumulated during load case 1.1.

The estimated fatigue life for the cable armouring, the copper screen and the conductor wires for all load cases exceeds $10^6$ load cycles above and beyond the loading applied during testing. Consequently, the probability of fatigue load failure for these components is very small.

*Friction effects.* The design allows the cores and associated components to slip when the cable is loaded. Allowing slip has the advantage of reducing maximum components stress by more evenly distributing loads within the cable structure [39]. However, when the cable is subjected to continuous loads, the relative slip between components may, in specific conditions, cause damage by wear, fretting or crushing. These effects, though driven by loads, are strongly dependent on physical material properties, load-deformation behaviour and surface conditions. These effects are notoriously difficult to model and consequently a high safety factor is normally applied during design. The mechanical cable models used at NSW are regularly calibrated using results of mechanical full and small-scale tests in order to estimate failure probability due to friction effects. Based on the above, the cross section analysis estimated, that a screen copper wire failures due to friction effects in the test conditions carries a medium likelihood.

*Failure likelihood for power cable components.* The outlined failure modes together with the FEA analysis and fatigue characteristics of the cable components allow an evaluation of the likelihood of failure for the individual components.

In order to classify the failure likelihood, a qualitative evaluation was carried prior to the physical tests, to estimate the failure likelihood as:

- *high* - Failure mode expected and predicted based on the numerical analysis
- *moderate* - Failure mode possible, based on numerical predictions and known failure modes
- *low* - Failure mode unlikely and not expected in the physical experiments

The assessment is shown in table 8, expressing the expected component failures after the bending tests. It should be noted here, that the cable specimen used is a static design submarine power cable which is exposed to a considerable amount of bending cycles during the tests, which represents the worst case scenario for operational loads.

The general failure modes occur through specific failure mechanisms which were replicated by the experimental conditions. Whilst the detailed physics and material processes are complex, they shall be briefly outlined here to explain the evaluation of failure likelihood.

*Over bending.* All marine power cables have a specified minimum bend radius (MBR), to which they can be bent without compromising their integrity. The bend restrictor CPS protects the cable from overbending and the associated calculated effective stress in the armouring wires for a MBR of 2.5m are estimated at 25% of the material Yield strength. As such the cable failure mechanism of overbending the through a single bending event was judged as low.

*Bending fatigue.* The repeated, cyclical bending of the cable subjects it to material fatigue. The repeated bending induces stress in the individual components and in particular the outer layers of copper and aluminum tape are exposed to repeated stresses that are below the material yield stress, but are large enough to induce fatigue damage. For the most severe loading case with $28^{circ}$ bending angle the Al sheath was exposed to up stresses up to 65% of its yield strength, whilst the copper tape was subject to up to 35% of its yield strength. The physical process of crack initiation and crack growth could not be monitored during the tests, but the microscopic analysis, shown in figure 10, reveals several fatigue cracks in the Al sheath which are up to $50\mu m$ long and are perpendicular to the maximum stress direction. The analysis of the copper tape, depicted in figure 11, shows a fatigue fracture with associated fatigue cracks that have propagated perpendicular to the maximum stress direction. The likelihood of both failure modes is also suggested by the S-N fatigue curves shown in figure 8. The test regime exceeds the nominal fatigue life in both cases. Therefore, the failure likelihood regarding bending fatigue is judged as high.

*Fretting.* Fretting is a form of wear that occurs between two metallic surfaces subjected to minimal relative oscillating motion (i.e. tens of microns). It is one of the possible crack initiation causes that may eventually produce fatigue fail-

Table 8: Von Mises effective stress in power cable metallic components as a percentage of material Yield strength, qualitative failure likelihood level and governing failure mode

| Component | Bending angle | | | Failure likelihood | Failure mode |
|---|---|---|---|---|---|
| | 28° | 14° | 7° | | |
| Armouring wires | 25% | <10% | <5% | low | Over bending |
| Aluminium sheath | 65% | <10% | <5% | high | Bending fatigue |
| Copper tape | 35% | <10% | <5% | high | Bending fatigue |
| Copper screen wires | <5% | <5% | <5% | moderate | Friction & fretting |
| Copper conductor wires | <5% | <5% | <5% | low | - |

ure. In the cable design, the copper screen wires are allowed to easily slip when the cable is subjected to bending loads in order to minimize stress concentration. Accordingly, the maximum effective stress acting on the copper screen wires as calculated by CableCAD is below 5% of the yield strength and consequently the likelihood of wires failure due to pure fatigue loading was considered low. However, the continuous wires slipping in response to the cable cyclic bending and consequently the continuous relative motion between wires as well as with the adjacent copper tape is expected to significantly increase the probability of failure due to friction effects including wear and fretting fatigue. Friction effects are not fully accounted for by CableCAD and the assessment is based on empirical methods.

### *3.3.2. Cable dissection*

The cable specimen was returned to NSW after the mechanical loading tests were completed. As loads applied during the test were significantly above the mechanical design limits of the cable, failures were expected. The cable was dissected at NSW's facilities in Germany. The tested cable had a total length of 5.4m. For the dissection, 2m length have been selected from the end that was connected to the DMaC headstock and thus was subjected to the largest cyclic bending stresses. The shortened section before dissection is shown in fig. 9.

*Serving, armouring and bedding.* Wear was evident on the cable serving PP yarns. Particularly significant in the section starting from the cable end connected to the DMaC headstock during testing, for a length of approximately 1m. Some instances of armour wires crossing were noticed. These were assumed to be the result of cable section cutting, transport and handling. No damage was identified on the armouring steel wires. No damage was noticed on the bedding layer.

*Fibre optic element.* No damage was noticed in the fibre optic element.

*Power core - outer sheath system.* There was no evidence of damage on the HDPE outer sheath. Cracks were distributed on the aluminium sheath surface for approximately 1.2m at headstock end section. They were concentrated on the left-right cross section quarters, while top-bottom quarters were mostly undamaged. The distribution of cracks clearly confirms the cable bending plane. An optical microscope image of the aluminium sheath, depicted in fig. 10, shows evidence of material cracks.

*Metallic screen.* Significant damage was found on both copper tape and screen wires (fig. 11). The copper tape had numerous fractures in the section subjected to bending as shown in fig. 11(a). Figure 11(b) shows multiple fatigue cracks developing from the copper tape edge as indicated by the red arrows.

Some evidence of fretting occurring on the copper screen wires in direct contact with the copper tape was also found. Only few copper screen wires failed due to fatigue loading. Figure 12 shows one example. The red arrow in the picture shows both the deep fretting initiated crack and crack propagation direction. No damage was noticed in the hygroscopic tapes placed between sheath and screen as well as between screen and insulation system.

*Insulation.* No damage was noticed in the insulation system.

*Conductors.* All conductor copper wires were found in good condition, although some signs of fretting were identified. Figure 13(a) shows signs of fretting occur-

ring at a contact point between copper conductor wires, while fig. 13(b) shows a superficial crack initiation on a conductor wire surface.

Some signs of wear could also be seen on the conductors' longitudinal semi-conducting hygroscopic tapes.

### *3.3.3. Failure/damage modes and impact on cable functionality*

The dissection of the cable after the substantial mechanical loading identified failures in the outer sheath of the power cores and the metallic screen. Some deterioration was also identified in the conductors. No further damage was identified in any other cable components after the test loading. This section presents a qualitative description of the causes of failure as well as a basic assessment of the failure impact on the cable functionality.

*Outer sheath system.* Failure of the aluminium sheath layer was expected in line with the mechanical modelling results. It has not been possible to fully establish if the aluminium sheath layer failure was due to overbending or fatigue as the extent of the damage was somewhat reduced by the strong bond between HDPE and aluminium sheath layers. The failure would significantly reduce the power core outer sheath system ability to act as total radial barrier to water penetration as some water diffusion is expected through the HDPE layer.

*Metallic screen.* Failures were noticed on the copper tape and copper wire screen layers. Evidence of fatigue failure was found in the copper tape. Again this was predicted by the mechanical model. Significant signs of fretting occurring between copper tape and screen wires were also found. Fretting initiated cracks have the effect to significantly accelerate fatigue failures. In this case, cyclic friction loads acting on the wires when slipping under bending were sufficient to produce a few screen wire failures. The probability of copper wire screen failure after test loading was estimated as medium following the cross section analysis. The dissection result confirms the uncertainties with this assessment and further justifies NSW present practice of applying high design safety factors when accounting for friction effects. The metallic screen failures observed are

not expected to significantly impact the cable functionality. However, they will have an impact on the overall system safety as it will affect the metallic screen ability to provide a return path to earth to any fault current or in case a short circuit should occur (e.g. due to a penetrating metallic object) between screen and conductor. It may also create the condition for the development of hotspots that could in turn compromise the integrity of polymeric elements [29].

*Conductor.* The conductors' wires slip due to bending and lead to a few fretting patches between conductor wires and some wear on the swelling tapes. However, no clues were found to suggest a significant risk of components functionality degradation under the test loading conditions.

## 4. Discussion of results

The bend restrictor has withstood considerable load regimes well in excess of any allowable design loads for offshore wind cable installations. The tests carried out dry mechanical loadings to accelerate the operational load conditions. The extreme 1:50 years load event was replicated with different acceleration factors to quantify the wear rates for different combinations of bending angles and tensile force. The maximum wear rate is considerably less than 1mm, with a original wall thickness of 8mm. This leaves some further margin to the critical wall thickness of 5mm. As such, the CPS has demonstrated its integrity during repeated high load events.

The mechanical loading applied to the cable sample during testing was also considerably above the stated design limits for static submarine power cables. The resulting component damage was reasonably in line with expectations, largely confirming present mechanical modelling and cross section analysis methodology. Additionally, as per normal practice, all data collected during this test will enable further calibration and strengthening of the model. None of the faults identified would cause a direct loss of service. However, they are expected to reduce the cable operating life and may affect the overall system safety.

The tests have been conducted in the spirit of O'Connor [40], who states that "... we must test to cause failures, not test to demonstrate successful achievement" in order to explore the reliability limits of novel applications. As such the tests have been highly accelerated provoking wear in the cable protection system and incipient failures in the power cable. A challenge of accelerated tests, however, is to ensure that the failure mode during the tests is not altered in respect to normal operating conditions [41]. Whilst accelerated testing is desirable for cost-effective testing it has its limitations in that not all operational conditions are ideally replicated. One limitation in the presented test programme are the different acceleration factors. Whilst the tension amplitude was accelerated, the magnitude of the bending moment was reduced, due the maximum bending moment that could be applied by the test rig. Ideally, the acceleration factors would be similar for consistency. In this regard, the axial tension was dominant in the tests. The main acceleration was however not the magnitude of the load, but the frequency of the loads. What would have been a diurnal tidal cycle frequency in the order of 6.25hours was accelerated by three orders of magnitude into 3-8s cycles. As such time-dependent failure modes are very difficult to infer from the given test setup. The mechanical failure modes under investigation can however be well replicated through repeated cycling. An ideal service simulation test would have also involved electrical tests. Unfortunately, this was not possible due to the available test equipment at the test facility. As a result, the paper cannot make any recommendations regarding electrical failure mechanisms and failure modes.

The highest acceleration was applied in load case 1.1, significantly overstressing the cable protection system and the cable itself. After 1,167 bending cycles, the CPS shell connected to the headstock mating piece failed due to excessive wear caused by abrasion with the stainless steel lip. This failure however was not seen as realistic failure mode. The force application for CPS exiting a monopile through a J-tube, exposed through scour and loaded with incident waves and tidal currents, would be different, i.e. distributed rather than point loaded. For the same reason it was decided to exclude the two shells connecting

to the moving headstock from the wear analysis, i.e. shells A29-A32, B29-B30 and C29-C30.

Regarding the observed cable damage, the point loading also exacerbates the wear mechanisms, as the bending is focused on a small region, rather than distributed across the free span of the cable. A further limitation of the tests is that the load cases were purely mechanical and thus ignore any effects that will be introduced when the cable is transmitting electricity. It is likely that electrical currents would contribute to further progressing incipient failures, as the potential for hotspots is well known [29].

The presented results for the cable damage also do not allow a precise inference when or by which load cycles the damage was caused, as it was not possible to dissect the cable between load regimes. Comparing the numerical stress analysis of the cable and with the experimental tests suggests that the majority of the observed damage is caused during the initial load regime. As such, it was possible to predict the over bending failure modes at the large displacement angles of $28^{circ}$. The bending fatigue failures for the individual components could also be predicted, although exact quantification is difficult, due to the uncertainties in crack initiation. Finally, fretting fatigue is difficult to predict, but it can be further evaluated through the identified contact points of the screen and conductor wires.

## 5. Conclusion & further work

This paper has demonstrated the rationale, implementation and results for an accelerated reliability test for an articulated pipe bend restrictor, protecting a static power cable. The tested conditions were accelerated extreme events from an estimated 1:50 years extreme load case that was accelerated between 1.25-6.67 times and repeated for up to 25,000 bending (50,000 tension) cycles. The cable protection system could demonstrate acceptable wear rates under the stated condition, offering confidence in its operational reliability. The static power cable sustained 77,000 bending cycles at different magnitudes yielding

limited cable damage that would not cause a direct loss of service.

However, whilst the worst case scenario was tested for both system it should be emphasised that any power cable deployment must ensure that no crushing, bend, torsional or tensile loads above stated limits would occur. Static design cables must also be protected from variable tensile and bending loads. When any significant variable loading during operations is expected, then dynamic power cables that include design solutions specifically aimed at withstanding variable loading should instead be selected. Whilst the articulated pipe bend restrictor offers protection against overbending, the cable is still able to bend, so in more dynamic conditions, such as floating offshore renewable energy applications, a combination of bend stiffener and bend restrictor should be sought to reduce the load exposure to the dynamic cable.

This paper is an initial step to quantify the degradation and failure processes for submarine power cables and associated additional protection systems. Potential future test improvements include a review and adjustment of the force application system in order to allow a more distributed load application. This could for example achieved with a 'cradle system' that is fed through the headstock in which the test specimen can rest. An extension of the test could also be achieved by including other protection systems and cable designs to identify the commonalities and differences across different design solutions for offshore marine applications. A greater number of samples would also allow to more regularly dissect the cable for damage analysis, allowing to map the damage contributions against the applied load conditions. Ideally this would be done for a representative fatigue load spectrum. Ultimately an extensive test programme could inform industry design standards for the protection of submarine power cables in offshore marine applications.

## Acknowledgements

The described test programme has received support from MARINET, a European Community - Research Infrastructure Action under the FP7 Capacities

Specific Programme. The first three authors would also like to acknowledge the support through the UK Centre for Marine Energy Research (UKCMER) under the SuperGen marine programme funded by the Engineering and Physical Sciences Research Council (EPSRC), grant EP/I027912/1 (www.supergen-marine.org.uk). The development of the component test rig was made possible through funding by the Peninsula Research Institute for Marine Renewable Energy (PRIMaRE), which was supported by the European Regional Development fund (ERDF) and the former South West Regional Development Agency (SWRDA).

[1] P. Higgins, A. Foley, The evolution of offshore wind power in the united kingdom, Renewable and Sustainable Energy Reviews 37 (0) (2014) 599 – 612. doi:10.1016/j.rser.2014.05.058.

[2] G. Corbetta, I. Pineda, J. Wilkes, J. Guillet, The european offshore wind industry - key trends and statistics 1st half 2014, Tech. rep., European Wind Energy Association (EWEA) (July 2014).

[3] Low Carbon Innovation Coordination Group, Technology Innovation Needs Assessment (TINA) Offshore Wind Power Summary Report, Summary report (February 2012).

[4] S. Faulstich, B. Hahn, P. J. Tavner, Wind turbine downtime and its importance for offshore deployment, Wind Energy 14 (3) (2011) 327–337. doi:10.1002/we.421.

[5] A. Zitrou, T. Bedford, L. Walls, K. Wilson, K. Bell, Availability growth and state-of-knowledge uncertainty simulation for offshore wind farms., in: 22nd ESREL conference, European Safety and Reliability Association, Amsterdam, 2013.

[6] J. Carroll, A. McDonald, D. McMillan, Failure rate, repair time and unscheduled O&M cost analysis of offshore wind turbines, Wind Energy (2015) in pressdoi:10.1002/we.1887.

[7] R. Lawler, Cables for offshore wind - steady as she goes, Materials World Magazine.
URL http://www.iom3.org/news/cables-offshore-wind-steady-she-goes?c=621

[8] L. Renforth, M. Seltzer-Grant, M. Foxall, Experiences in the condition monitoring and testing of subsea high voltage cables in the UK offshore industries, in: Proc. TechCon Conference, 2012.
URL http://www.hvpd.co.uk/media/pdf/technical/experiences-in-the-monitoring-testing-sub

[9] T. Boehme, D. J. Robson, Offshore wind farm cabling: incidents and required learning, Proceedings of the ICE - Forensic Engineering 165

(2012) 185–197(12).
URL http://www.icevirtuallibrary.com/content/article/10.1680/feng.12.00013

[10] BS EN 62506:2013 methods for product accelerated testing, (2013).

[11] S. D. Weller, P. Thies, T. Gordelier, P. D. P, L. Johanning, The role of accelerated testing in reliability prediction, in: Proc. 1th European Wave and Tidal Energy Conference EWTEC, Nantes, France,, 2015.
URL http://hdl.handle.net/10871/18315

[12] A. Rodriguez, S. D. Weller, J. Canedo, R. Rodriguez, V. G. de Lena, P. Thies, D. Parish, L. Johanning, A. Leao, Performance comparison of marine renewable energy converter mooring lines subjected to real sea and accelerated loads, in: Proc. 11th European Wave and Tidal Energy Conference EWTEC, Nantes, Paris,, 2015.
URL http://hdl.handle.net/10871/18313

[13] M. Marta, S. Mueller-Schuetze, H. Ottersberg, D. Isus, L. Johanning, P. Thies, Development of dynamic submarine mv power cable design solutions for floating offshore renewable energy applications, in: Proc. Jicable'15 - 9th Int. Conference on Insulated Power Cables, Paris, France,, 2015.
URL http://hdl.handle.net/10871/18314

[14] F. P. Nasution, S. Sævik, J. K. Gøsteen, Finite element analysis of the fatigue strength of copper power conductors exposed to tension and bending loads, International Journal of Fatigue 59 (2014) 114 – 128. doi:10.1016/j.ijfatigue.2013.09.009.

[15] F. P. Nasution, S. Sævik, J. Gjøsteen, Fatigue analysis of copper conductor for offshore wind turbines by experimental and FE method, Energy Procedia 24 (2012) 271 – 280, selected papers from Deep Sea Offshore Wind R&D Conference, Trondheim, Norway, 19-20 January 2012. doi:10.1016/j.egypro.2012.06.109.

[16] F. P. Nasution, S. Sævik, S. Berge, Experimental and finite element analysis of fatigue strength for 300mm$^2$ copper power conductor, Marine Structures 39 (2014) 225 – 254. doi:10.1016/j.marstruc.2014.07.005.

[17] S. Vize, C. Adnitt, R. Staniland, J. Everard, A. Sleigh, R. Cappell, S. McNulty, M. Budd, I. Bonnon, J. Carey, Review of cabling techniques and environmental effects applicable to the offshore wind farm industry, Tech. rep., Department for Business Enterprise & Regulatory Reform (BERR), London, UK (2008).

[18] M. P. Sharples, Offshore electrical cable burial for wind farms: State of the art, standards and guidance & acceptable burial depths, separation distances and sand wave effect, Tech. rep., Bureau of Ocean Energy Management, Regulation and Enforcement (2011).

[19] R. Beindorff, L. van Baalen, Theory on submarine power cable protection strategies, in: Proc. of EWEA 2013, European Wind Energy Association, 2013.

[20] P. R. Thies, L. Johanning, G. H. Smith, Towards component reliability testing for marine energy converters, Ocean Engineering 38 (2-3) (2011) 360 – 370. doi:10.1016/j.oceaneng.2010.11.011.

[21] P. R. Thies, L. Johanning, T. Gordelier, Component reliability testing for wave energy converters: Rationale and implementation, in: Proc. of 10th European Wave and Tidal Energy Conference EWTEC, Aalborg, Denmark, 2013.

[22] P. R. Thies, L. Johanning, T. Gordelier, A. Vickers, S. Weller, Physical component testing to simulate dynamic marine load conditions, in: Proc. of 32nd ASME Int. Conference on Ocean, Offshore and Arctic Engineering (OMAE), no. OMAE2013-10820, Nantes, France, 2013. doi:10.1115/OMAE2013-10820.

[23] P. R. Thies, L. Johanning, K. Karikari-Boateng, C. Ng, P. McKeever, Component reliability test approaches for marine renewable energy, Proc. of the Institution of Mechanical Engineers, Part O: Journal of Risk and Reliability 229 (5) (2015) 403–416. doi:10.1177/1748006X15580837.
URL http://hdl.handle.net/10871/18321

[24] Orcina, OrcaFlex Manual, Daltongate, Ulverston, Cumbria, LA12 7AJ, UK, version 9.5a (2013).
URL www.orcina.com

[25] CIGRE, Electra 171 - recommendations for mechanical tests on sub-marine cables, Tech. rep., International Council on large electrical systems (1997).
URL http://www.cigre.org/

[26] NSW, NSW Submarine Power Cables (2011).
URL www.nsw.com

[27] CENELEC, HD 620 S2 - Distribution cables with extruded insulation for rated voltages from 3.6/6(7.2) kV up to and including 20.8/36(42) kV, Tech. rep., European Committee for Electrotechnical Standardization (2010).

[28] IEC, IEC 60228 - Conductors of Insulated cables (2004).

[29] IEC, IEC 60502-2 - Power cables with extruded insulation and their accessories for rated voltages from 1kV up to 30kV (2005).

[30] GOM, Atos triple scan, accessed 22/10/2014.
URL http://www.gom.com/metrology-systems/system-overview/atos-triple-scan.html

[31] Cable CAD, Structural solutions.
URL www.cablecad.com

[32] R. Knapp, S. Das, Finite element stress analysis of cables, in: OCEANS'99 MTS/IEEE. Riding the Crest into the 21st Century, Vol. 2, IEEE, 1999, pp. 1026–1033.

[33] W. C. Young, R. G. Budynas, Roark's formulas for stress and strain, Vol. 7, McGraw-Hill New York, 2012.

[34] J. Wolfram, On assessing the reliability and availability of marine energy converters: The problems of a new technology., Proceedings of the Institution of Mechanical Engineers, Part O: Journal of Risk and Reliability 220 (1) (2006) 55–68.

[35] P. R. Thies, L. Johanning, G. H. Smith, Assessing mechanical loading regimes and fatigue life of marine power cables in marine energy applications, Special Issue Proc. of the Institution of Mechanical Engineers, Part O, Journal of Risk and Reliability 226 (1) (2012) 18–32. doi:10.1177/1748006X11413533.

[36] M. A. Miner, Cumulative damage in fatigue, Journal of Applied Mechanics 12 (1945) A159–A164.

[37] R. W. Hertzberg, Deformation and fracture mechanics of engineering materials, Vol. 89, Wiley, 1996.

[38] M. Murphy, The engineering fatigue properties of wrought copper, Fatigue & Fracture of Engineering Materials & Structures 4 (3) (1981) 199–234.

[39] K. Feyrer, Wire Ropes: Tension, Endurance, Reliability, Springer, 2007.

[40] P. D. T. O'Connor, Practical reliability engineering, 4th Edition, Wiley, 2008.

[41] S. Lydersen, M. Rausand, A systematic approach to Accelerated Life Testing, Reliability Engineering 18, 4 (1987) 285–293.

## List of Figures

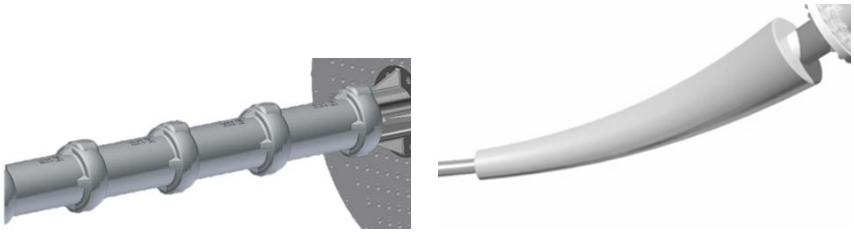

(a) Bend restrictor (b) Bend stiffener

Figure 1: Mechanical cable protection systems

(a) Setup overview

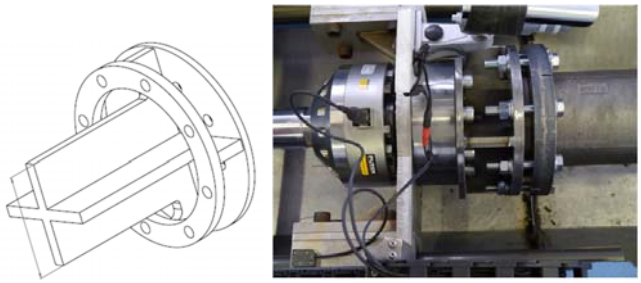

(b) Tailstock

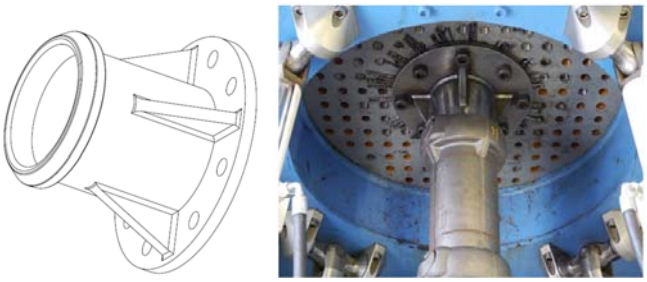

(c) Headstock

Figure 2: Experimental setup of cable/cable protection system at Dynamic Marine Component test rig, length of specimen is 5.4m

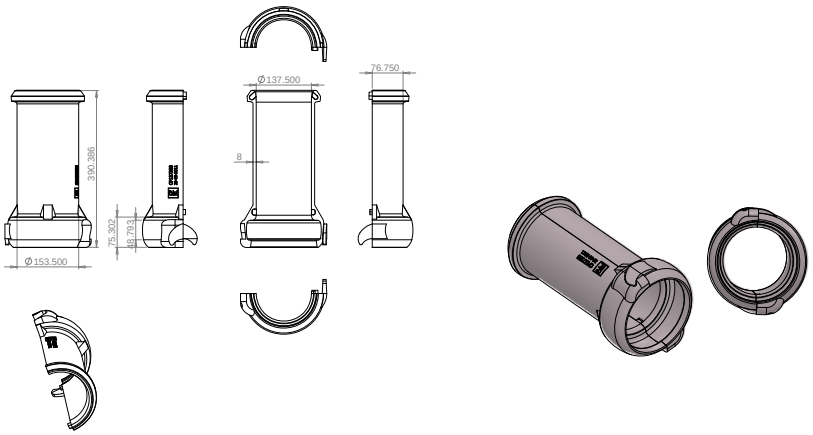


(a) Dimensions individual shells (b) Assembled shell

Figure 3: CPNL articulated pipe bend restrictor system

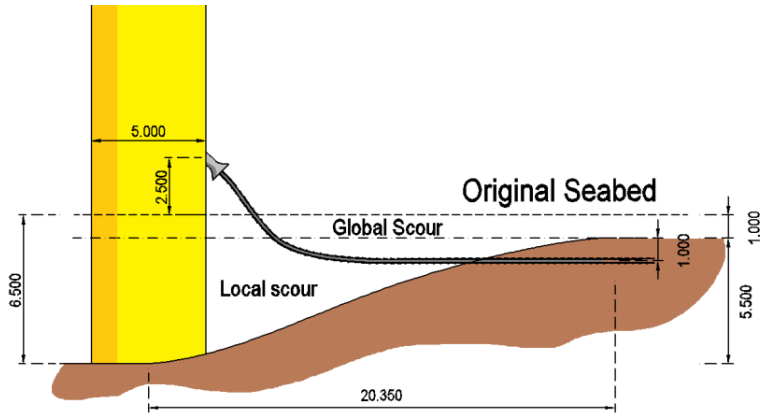


Figure 4: Model setup for maximum load case in scour condition, cable and cable protection system are fed into the tower via a J-tube

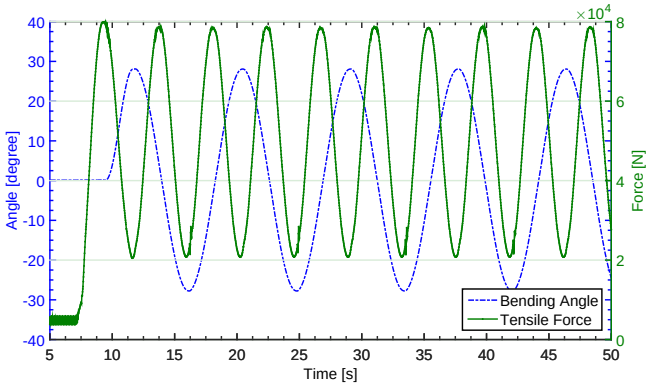


Figure 5: Load case 1.1 - Extract of recorded time series.

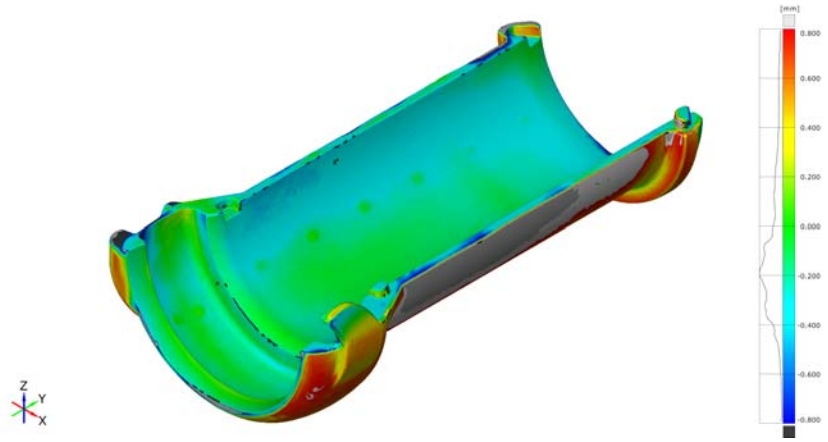

Figure 6: Example of 3D scan results, showing deviation from tested shell in comparison with CAD.

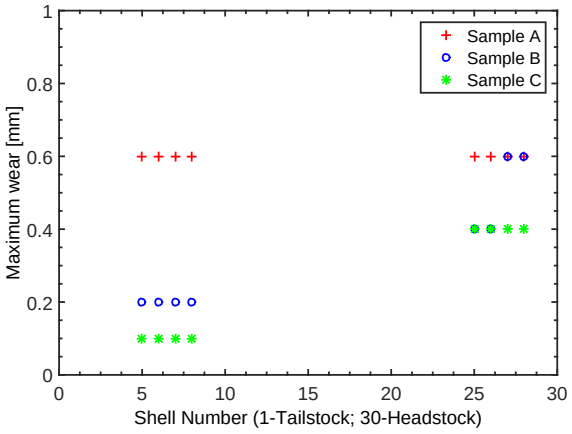


Figure 7: Summary of 3D scan results, showing scan deviation results for shell A28. Comparison is made with CAD file against post-test scan of shell.

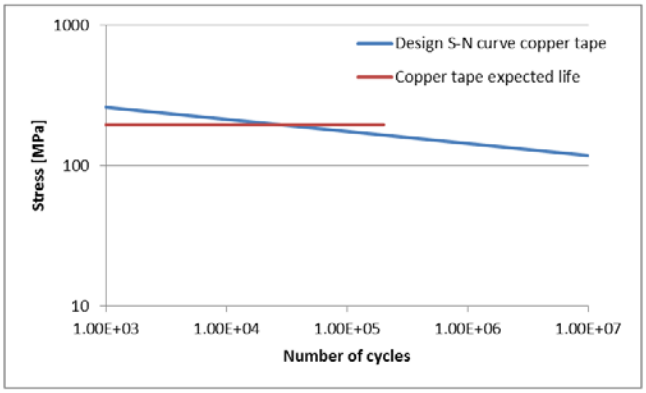


(a) Copper tape

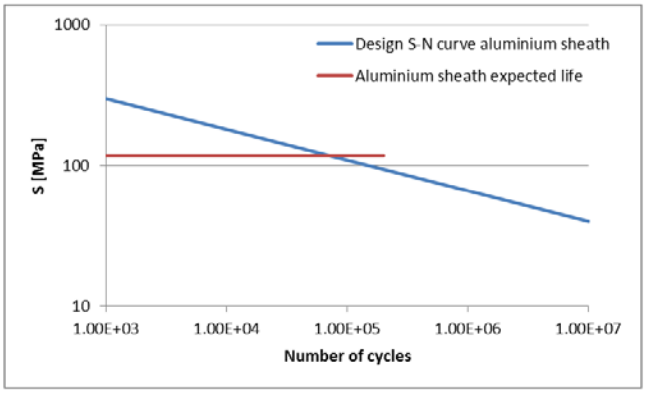


(b) Aluminium Sheath

Figure 8: Estimated fatigue life for 28° headstock y-angle, showing copper tape (8(a), [38]) and aluminium sheath (8(b), [37]).

Figure 9: Power cable section before dissection and analysis. The arrow indicates end mounted to test rig headstock.

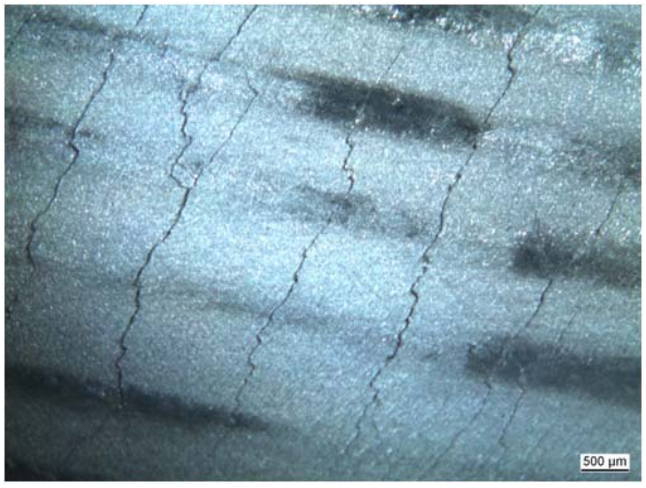


Figure 10: Optical microscope view of aluminium sheath internal surface showing fatigue cracks caused by cyclic cable bending.

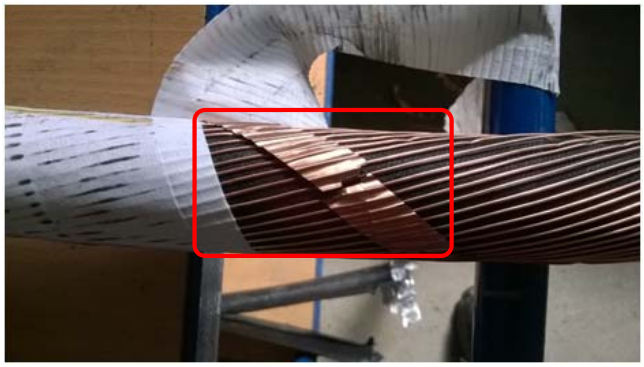

(a) Fatigue failure

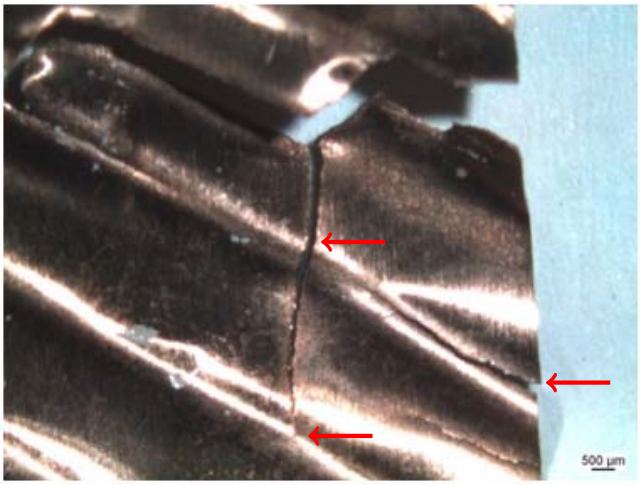


(b) Fatigue cracks

Figure 11: Copper tape damage identification

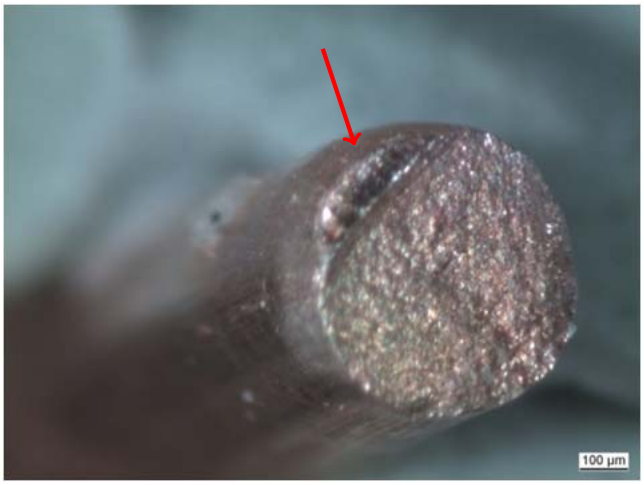


Figure 12: Copper screen wire cross section failed due to fretting fatigue

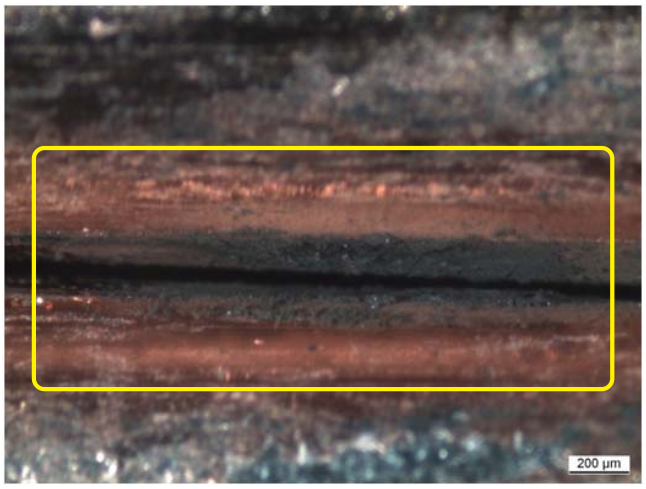


(a) Fretting between two conductor wires

(b) Fretting on conductor wire surface

Figure 13: Conductor wire fretting